Design and Fabrication of Gas Sensors by using Heterostructured Nanomaterials

SUMMARY SUBMITTED FOR THE AWARD OF THE DEGREE OF

Doctor of Philosophy

in

Physics

Submitted by

Ajeet Singh

Enrolment no.- 675/15

Under the supervision of

Prof. (Dr.) Bal Chandra Yadav

DEPARTMENT OF PHYSICS

SCHOOL OF PHYSICAL & DECISION SCIENCES

BABASAHEB BHIMRAO AMBEDKAR UNIVERSITY

(A CENTRAL UNIVERSITY) (NAAC-A^{++} ACCREDITED)

LUCKNOW-226025 (U.P.) INDIA

2024

SUMMARY

Design and Fabrication of Gas Sensors by using Heterostructured Nanomaterials

At present, atmospheric pollution is a worldwide issue due to various human activities such as the burning of hydrocarbons in the form of numerous fuels through industrial, vehicle, automobile, and domestic sources which emit harmful and toxic gases [1]. These toxic gases are harmful to human beings as well environment. So, the monitoring of toxic and harmful gases is quite necessary [2]. For this purpose, highly sensitive, self-powered, and robust gas sensors are required. This motivation is driven by the significance of gas sensor technology in a diverse number of areas such as environmental monitoring, the security sector, medical diagnostics, and food industries [2, 3].

The numerous kinds of gas sensor technology that span the capability to detect various types of gases. Fig. 1(a) illustrates the different types of gas sensing devices such as optical, electrochemical, capacitive, acoustic, and resistive sensors [4]. Among them, resistive type gas sensors have been widely investigated due to their unique advantages such as excellent sensitivity, cost-effectiveness, easy fabrication, real-time detection, facile integration, highly stable, compact, and portable [5]. At present, in resistive-type gas sensing devices different types of nanostructured materials are widely used as shown in Fig. 1(b). These nanomaterials include metal oxide semiconductors (MOS), carbon nanotubes (single and multi-walled), 2D materials, conducting polymers, graphene and its derivatives (graphene oxide (GO) and reduced graphene oxide (rGO)), and metal-organic frameworks (MOFs) etc. In comparison to MOS, other nanostructures such as carbon nanotubes are relativity expensive and have poor selectivity [6]. Graphene and its derivatives-based gas sensors are prone to conglomeration between layers and have low yields and high prices. Also, conducting polymers-based gas sensors possess low stability, long recovery time, and poor mechanical strength [7]. MOSs are promising gas-sensing materials due to their easy fabrication, highly sensitive, robust, miniaturized, and stable etc. However, the binary MOS gas sensors had poor selectivity and operated at high temperatures. High operating temperature, low sensitivity, and poor selectivity are the problems of binary MOS-based gas sensors [8]. These shortcomings are

overcome due to the doping of noble metals, sensitization, functionalization, a combination of more than two metal oxides, and MOS-based heterostructures [9]. Interesting characteristics of heterostructures include the formation of heterojunctions, which separate charge carriers, greater active sites, spill-over effects, etc. making potential candidates used for the detection of gases [10, 11]. Fig. 1(c) represents the general type of heterostructures including mixed, core-shell, multilayer, decorated, branched, and hollow etc.

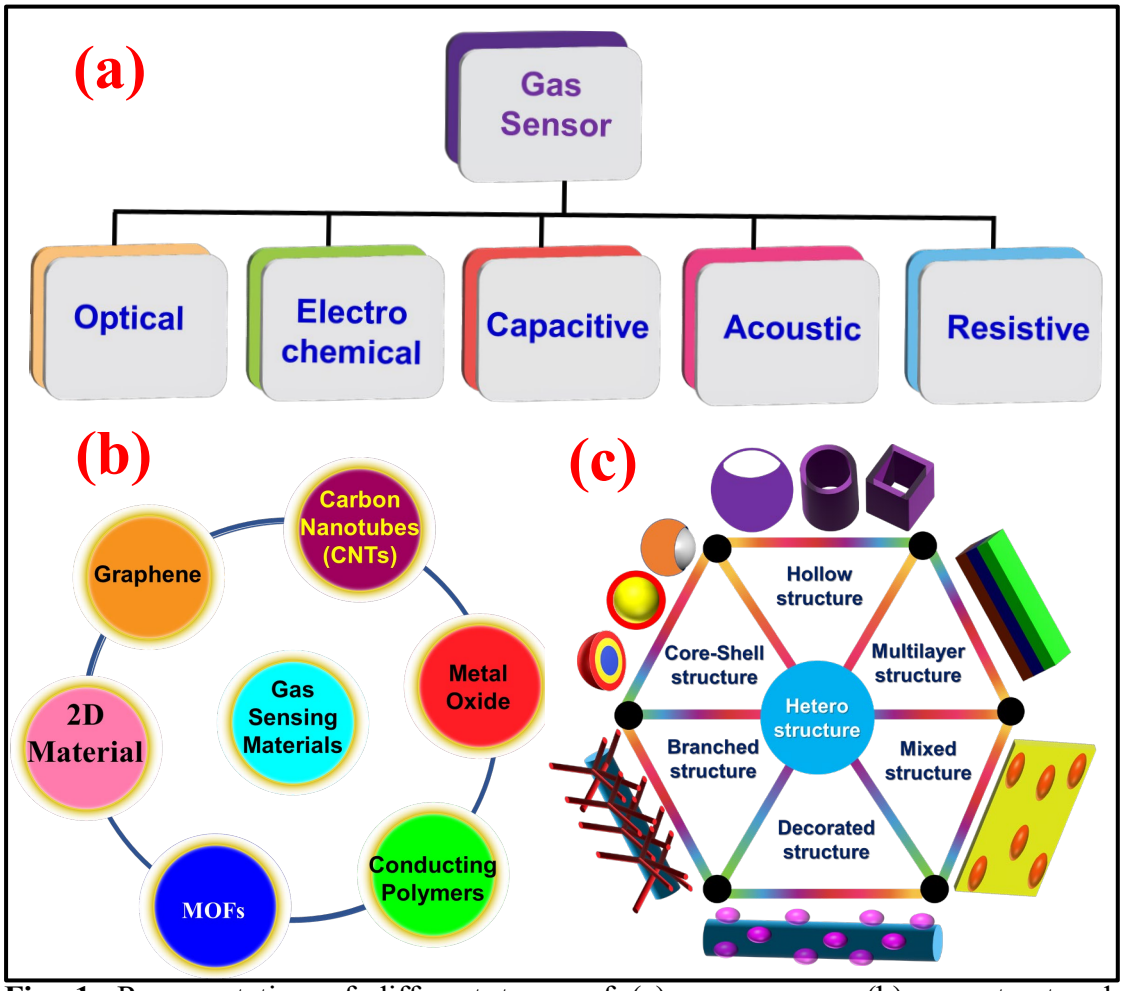

Fig. 1. Representation of different types of (a) gas sensors, (b) nanostructured materials, and (c) heterostructures categories.

MOS heterostructures-based sensing devices are used for the detection of different analytes, but there are still numerous findings and research which are to be achieved to recognize entirely the opportunities of these materials. All the chapters are summarised as follows:

Chapter 1 deals with the description of MOS-based heterostructures, their types, properties, and synthesis methods. In this chapter, various kinds of gas sensors

such as thermal, electrochemical, optical, and chemiresistive sensors are discussed. The general gas sensing mechanism of n-type and p-type semiconductors based on space charge layer, Debye length, and grain size were briefly explained. Also, variations in the resistance of n-type and p-type semiconductors after exposure to oxidizing/reducing gases were explored. Various preparation techniques used to synthesize different heterostructures were described. Additionally, the role of heterojunction (p-n, n-n, and p-p) and their gas sensing mechanism were explained. This chapter describes various kinds of detection techniques based on the operation of resistive-type gas sensors. These techniques are including such as high operating temperature and self-powered system. Self-powered gas sensors operated without an external power source using nanogenerators (TENG and PENG) along with opportunities and challenges in MOS heterostructures-based gas sensors have been discussed.

Chapter 2deals with the preparation of undoped and indium-doped SnO_2 nanomaterials by using sol-gel route. In this investigation, a highly responsive and cost-effective liquified petroleum gas (LPG) sensor using indium-doped SnO_2 nanospheres operable at room temperature (RT) has been fabricated. The synthesized nanomaterials were characterized to study surface morphology, elemental compositions, crystal structure, phase formation, optical absorption, etc through SEM, EDS, XRD, TEM, Raman, FTIR and UV-visible spectroscopy.

After the doping of indium, the properties of nanomaterials were changed. The crystallite size of SnO_2 and In/SnO_2 nanomaterials were estimated as 10.60 nm and 7.53 nm respectively. Additionally, from SEM analysis the average particle size of SnO_2 and In/SnO_2 nanospheres were around ~35.25 nm and ~29.96 nm, respectively. Fig. 2(a) shows the SEM micrograph of In/SnO_2 nanospheres. The optical band gap was estimated by UV-visible absorption spectrum and found to increase because of decreasing the particle size of In/SnO_2 nanosphere. The direct optical energy bandgaps for SnO_2 and In/SnO_2 were found as 3.72 eV and 3.87 eV respectively as shown in Fig. 2(b).

The sensing characteristics of In/SnO_2 thin film have been studied and it was found quite useful to detect the concentrations below LEL (0.5-2.0 vol%). The LPG sensing characteristics of In/SnO_2 film are shown in Fig. 2(c). The maximum sensor response of undoped and Indium-doped SnO_2 was estimated as 1.67 and 4.65 for 2.0

vol% LPG. Thus, the sensor response of Indium-doped SnO_2 is ~5.37 times higher than undoped SnO_2sensor.The sensitivity of the pristine SnO_2 and Indium-doped SnO_2 films were found ~0.386 sensor response/vol% and 2.087 sensor response/vol%, respectively as shown in Fig. 2(d). Also, the sensitivity of Indium-doped SnO_2 thin film was found ~5.40 times higher than SnO_2 thin film. In comparison to bare SnO_2 nanomaterials, the Indium-doped SnO_2 sensor showed high sensing performance. Also, the minute effect of humidity on gas sensing was observed.

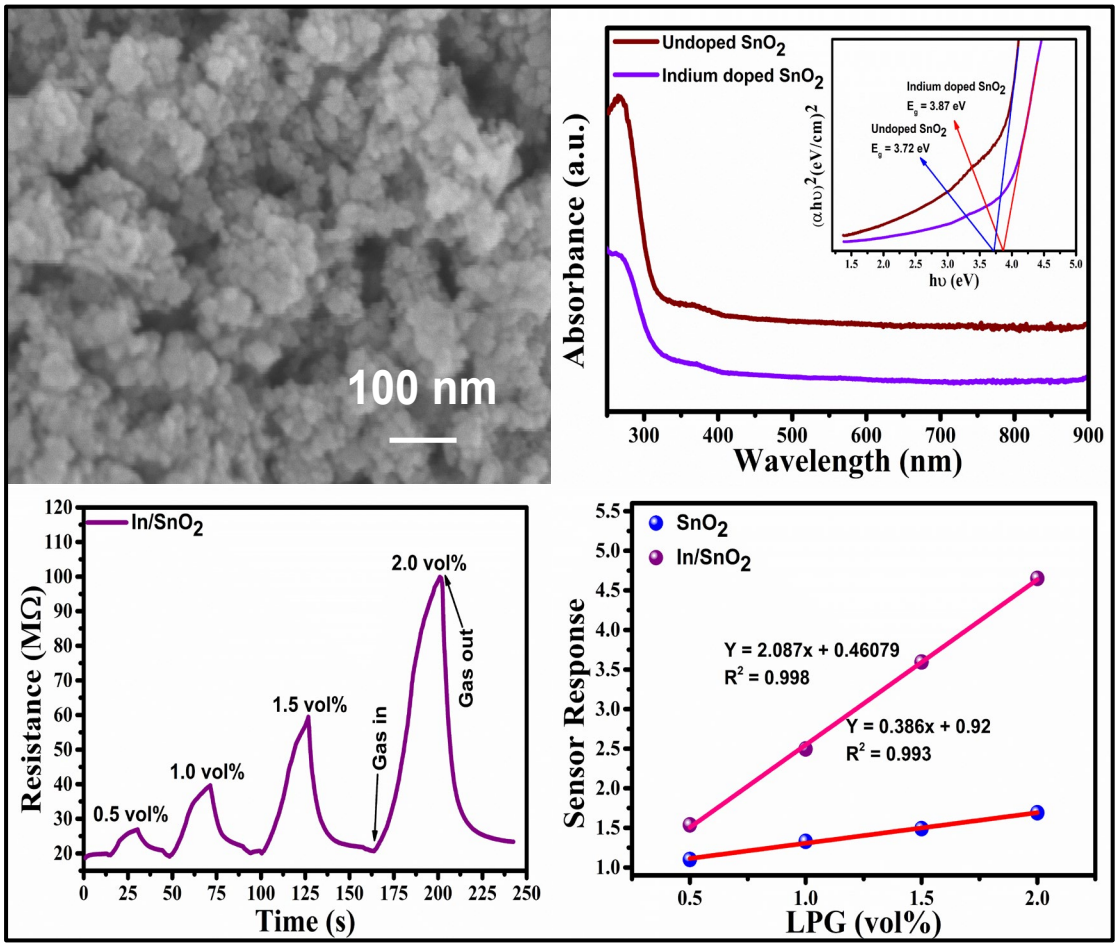

Fig. 2. SEM micrograph of(a**)** In/SnO_2, (b) UV-visible absorption spectra with inset of Tauc's plot, (c) transit LPG sensing of In/SnO_2 sensor, and (d) response curve towards different concentration 0.5-2.0 vol%.

Chapter 3 describes the preparation of ZnO/NiO (1D/3D) heterostructures by using the green technique. In this work, Azadirachta Indica (Neem) leaf extract was used for the preparation of ZnO, NiO, and ZnO/NiO nanomaterials. Plant-mediated green synthesis of nanoparticles is a cost-effective, eco-friendly, time-efficient, and innovative technique [12]. The morphological investigation of ZnO and NiO was done by SEM and confirms the formation of nanorods and nanocubes whereas,

ZnO/NiO nanocomposite clearly observed that the two morphologies such as nanorods and cubes exist. The SEM micrograph of ZnO/NiO heterostructures is shown in Fig. 3(c). The structural properties were analysed by X-ray diffractometer. The XRD pattern of ZnO/NiO heterostructures reveals the polycrystalline nature in which ZnO and NiO have hexagonal and cubic phase structures which was also confirmed by the Rietveld refinement analysis.

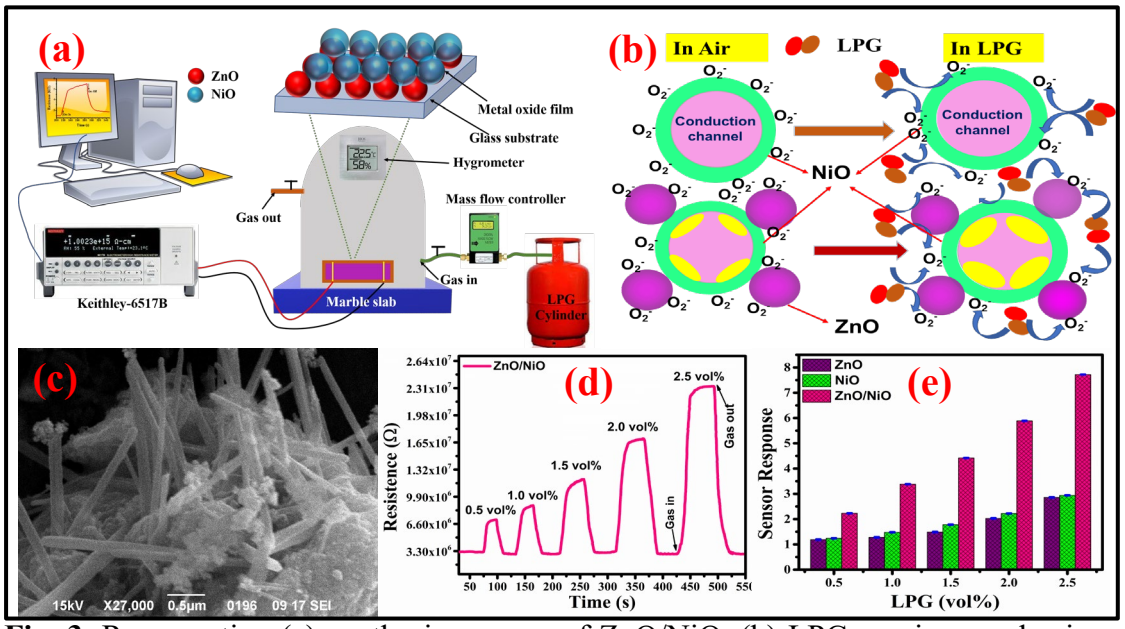

Fig. 3. Representing (a) synthesis process of ZnO/NiO, (b) LPG sensing mechanism (c) SEM micrograph, (d) transit LPG sensing characteristics, (d) sensor response curve.

The optical properties were analysed by the UV-visible absorption spectrum. Energy band gaps of ZnO, NiO, and ZnO/NiO heterostructures were estimated by Tauc's plot and found to be 3.62, 3.81 eV and 3.71 eV, respectively. The schematic of LPG sensing measurement setup is shown in Fig. 3(a). LPG sensing measured up to 0.5-2.5 vol% at room temperature as shown in Fig. 3(d). The bar graphs of sensor response of ZnO, NiO, and ZnO/NiO sensors are depicted in Fig. 3(e). The maximum sensor response of ZnO/NiO heterostructure-based sensor was found 7.72 at 2.5 vol% which is 2.6 times higher than pure ZnO and NiO. The fast response and recovery times of ZnO/NiO were found to be 7.83 s and 11.01 s, respectively at 0.5 vol% LPG. Also, the ZnO/NiO is highly selective for LPG in comparison to other analytes like ethanol, acetone, ammonia, and CO_2 etc. Since the ZnO/NiO heterostructures can be effectively used for the detection of LPG at room temperature. Also, in this chapter, the DFT analysis of ZnO/NiO without and with LPG interaction was performed by

B3LYP/LAN2DZ basis set for a better understanding of the sensing phenomenon. The schematic of LPG sensing mechanism of ZnO/NiO heterostructure is shown in Fig. 3(b).

Chapter 4 involves the fabrication of photo-enhanced CO_2 gas sensors based on SnO_2@CdO decorated heterostructure. The synthesis process of SnO_2@CdO heterostructures is shown in Fig. 4(a). The nanomaterials were investigated using XRD, SEM, TEM, XPS etc.

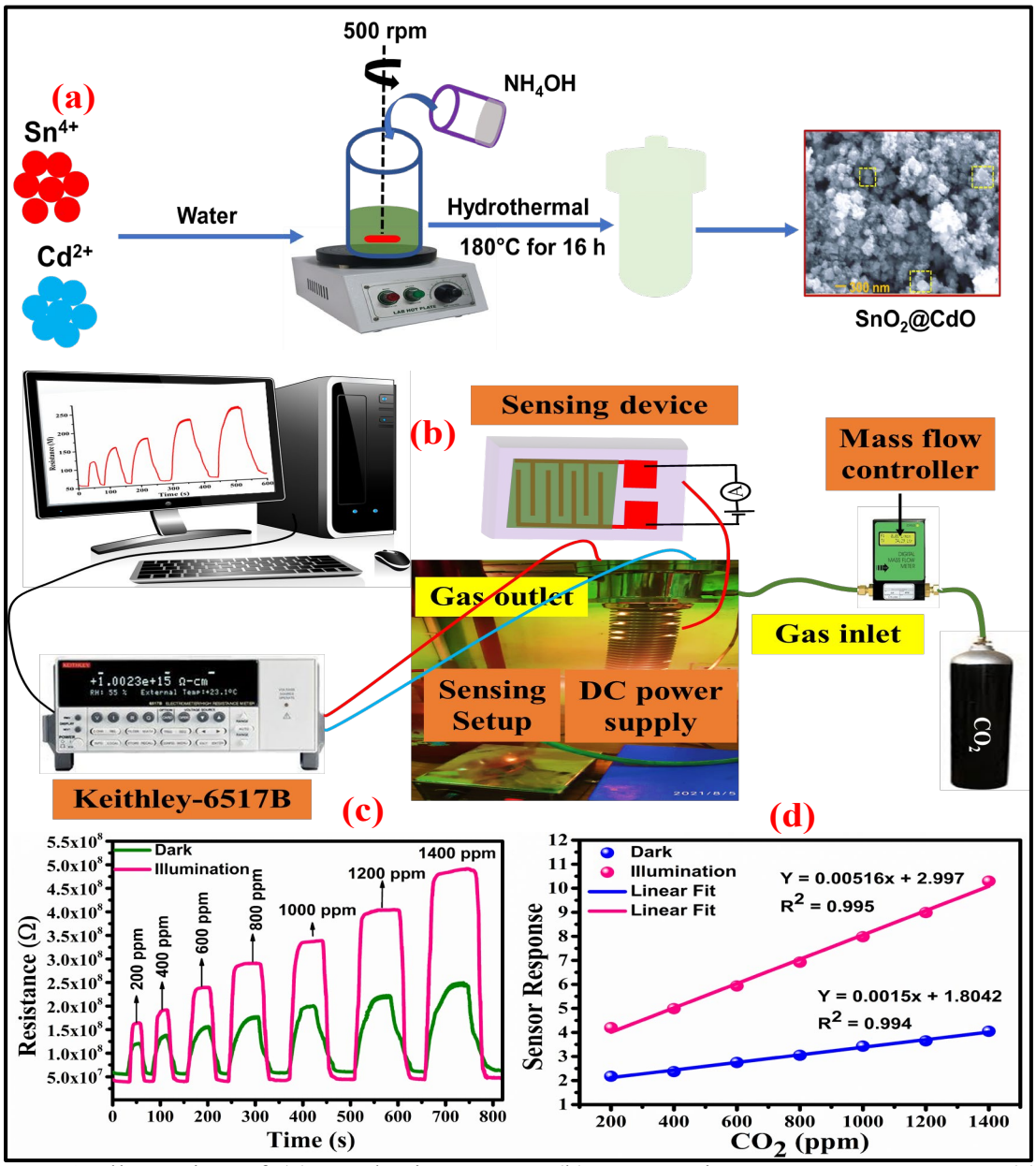

Fig. 4. Illustration of (a) synthesis process, (b) gas sensing measurement setup, (c) transit CO_2 gas sensing in the dark and illumination for different concentrations, and (d) sensor response curve.

The detection of CO_2gas was performed at room temperature towards 200-1400 ppm in dark and illumination of 30 mW/cm^2. Fig. 4(b) shows the gas sensing measurement setup. The results of CO_2 gas sensing characteristics were evaluated in 30 mW/cm^2 visible light source and found to be excellent. The CO_2 sensing characteristics at different concentrations are shown in Fig. 4(c) in dark and illumination. The sensor response curve of SnO_2@CdO heterostructure is shown in Fig. 4(d). The maximum sensor response of the light-induced CO_2 gas sensor was found to be 10.29 towards 1400 ppm of CO_2 at RT within 18.53 s which is 2.5 times higher than without illumination. Also, the sensitivity of sensor in irradiation of light was found to be 3.44 times higher than in the dark. The SnO_2@CdO decorated heterostructure was formed n-n heterojunction and the irradiation of light enhances the surface adsorption/desorption of CO_2 gas to the sensing surface. The selectivity was checked in the presence of various analytes such as ethanol, acetone, ammonia and LPG. Further, the DFT analysis provided useful information that the SnO_2@CdO is very effective and highly sensitive for CO_2 detection. This study affords a rational way for the design and fabrication of resistive type CO_2 gas sensors operated at room temperature and capable of outdoor monitoring of CO_2.

Chapter 5 deals with the comparative analysis of resistive and self-powered CO_2 gas sensors. In this work, CeO_2, CdS, and CeO_2/CdS nanospheres were prepared via hydrothermal method. Also, the self-powered gas sensing system was designed by using CeO_2/CdS heterostructured-based triboelectric nanogenerator (TENG) as shown in Fig. 5(a). The surface morphological investigation was done by FESEM and observed to random growth of nanospheres. The nanospheres of CeO_2 and CdS were found to be 10-30 nm and 20-60 nm, respectively. Additionally, the distribution of elements is confirmed by the elemental mapping. The XRD pattern of pure CeO_2 and CdS has a single crystalline cubic and hexagonal crystal structure whereas the CeO_2/CdS nanocomposite has a polycrystalline nature. The average crystallite size of CeO_2, CdS, and CeO_2/CdS nanocomposite were estimated by Scherrer's formula and found to be 16.31, 16.62, and 20.54 nm respectively. The energy band gaps of CeO_2, CdS, and CeO_2/CdS nanospheres were estimated from Tauc's plot as 2.92 eV, 2.52 eV, and 2.63 eV, respectively. The oxidation states of elements and interface analysis were performed by X-ray photoelectron electron spectroscopy. XPS confirmed the existence of Cd^{2+}, S^{2+}, Ce^{2+}, and O^{2-} oxidation

states of elements. It also confirmed the formation of n-n heterojunction in CeO_2/CdS heterostructure. The CO_2 gas sensing was studied at room temperature toward various concentrations (250-1000 ppm) and the sensing measurement setup is shown in Fig. 5(b). The CO_2 sensing characteristics of self-powered and resistive sensors are shown in Fig. 5(c, d). The sensor response (30 at 1000 ppm) and sensitivity (0.034 sensor response/ppm) of the self-powered sensor showed almost 10 times in comparison to the resistive type sensor. The self-powered CO_2 sensor not only shows the high sensor response but also provides the power for the sensor measurement process by converting mechanical energy into electrical energy (by finger tapping) without any external power source. The sensor was operated with TENG that generated an output voltage and current of ~90 V and 9.6 μA, respectively which is quite high till now in comparison to as-fabricated heterostructure-based nanogenerators. Moreover, the self-powered sensor showed 1.835/0.835 s response/recovery times at 250 ppm of CO_2. Also, the outstanding selectivity of the sensor for CO_2 among the analytes, acetone, ethanol, LPG etc. was observed.

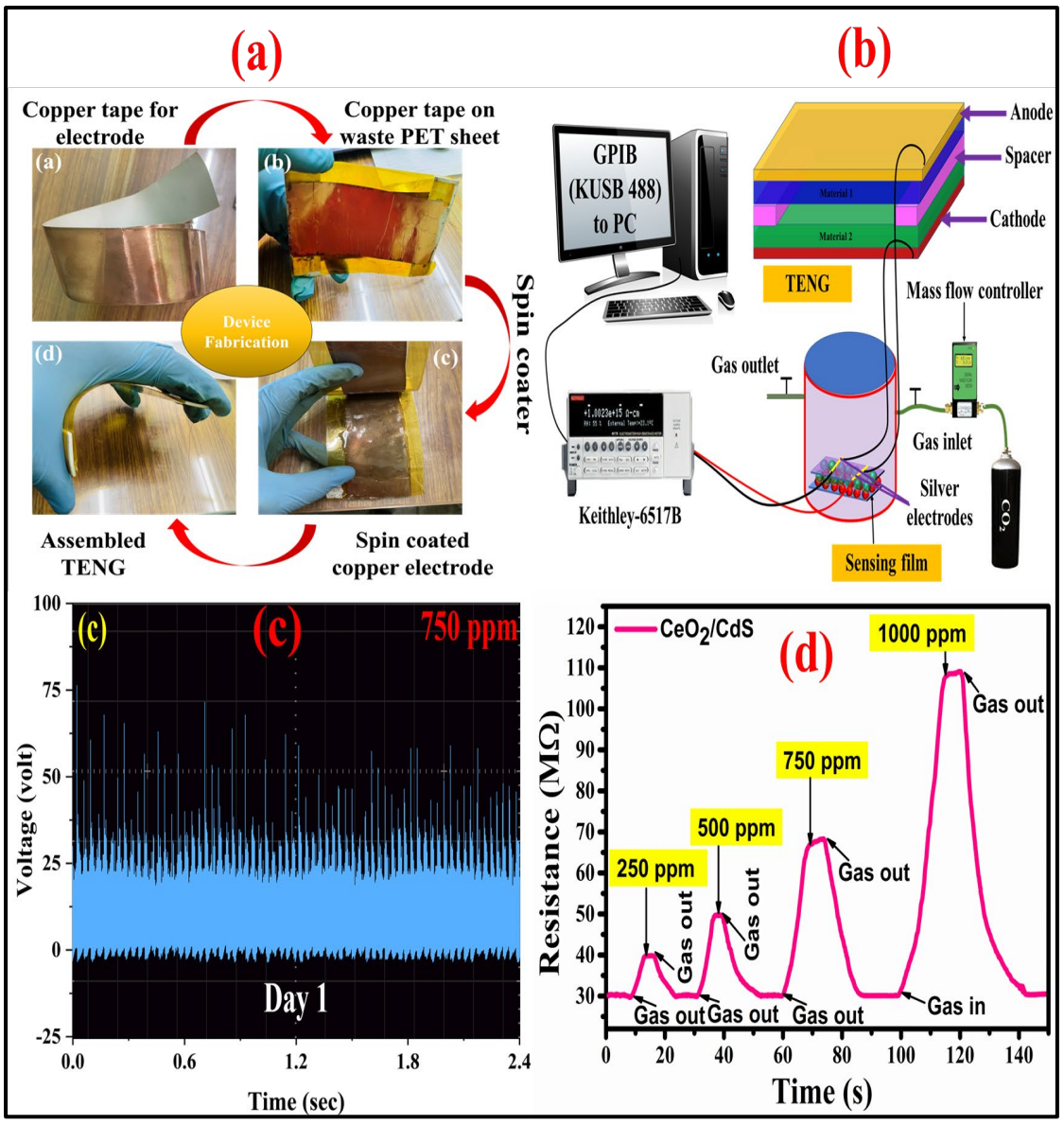

Fig. 5. (a) Fabrication of TENG, (b) Passive self-powered TENG-based CO_2 gas sensing measurement setup, (c) Self-powered CO_2 gas sensing characteristics at 750 ppm, and (d) Transit CO_2 gas sensing characteristics of resistive type CeO_2/CdS sensor.

Chapter 6 deals with a unique, cost-effective, and quick method for the detection of triethylamine (TEA) gas. A concept for the preparation of MOFs derived heterostructure materials for the fabrication of high-performance gas sensors was proposed. The ZIF-8 derived Ag@$ZnWO_4$/ZnO branched heterostructures have been synthesised by cost-effective low-temperature solvothermal followed by an annealing process in air and the synthesis process is shown in Fig. 6(a). The surface morphological investigation was done by SEM and confirmed the $ZnWO_4$ nanorods grown on ZnO whiskers. Also, the X-ray mapping was carried out to receive more

information about the composition and element distributions of Ag@$ZnWO_4$/ZnO composite. Further, the topographical analysis was executed by TEM and diameters of $ZnWO_4$ nanorods were observed around 10-30 nm. The selected area diffraction pattern (SAED) confirmed the diffraction planes of ZnO and $ZnWO_4$in both phases exist. The interplanar spacing of diffraction planes of $ZnWO_4$ and ZnO were calculated by ring pattern. The inter-planar spacing was found to be 2.953Å for (111) plane of $ZnWO_4$ and 2.489 Å for (101) plane of ZnO, respectively. The XPS analysis was performed to estimate the chemical composition and oxidation states. The XPS analysis revealed the existence of $Zn2^+$, W^{4+}, Ag^{2+}, and O^{2-} oxidation states. The structural properties were analysed by XRD and confirmed the phase structures of ZIF-8, ZnO, and $ZnWO_4$ which are found cubic, hexagonal, and monoclinic, respectively. Also, the Rietveld refinement was carried out for structural parameters in this chapter. The average crystallite size of ZnO, $ZnWO_4$ and ZIF-8 derived Ag@$ZnWO_4$/ZnO were estimated to be 17.80 nm, 15.50 nm, and 21.51 nm respectively.

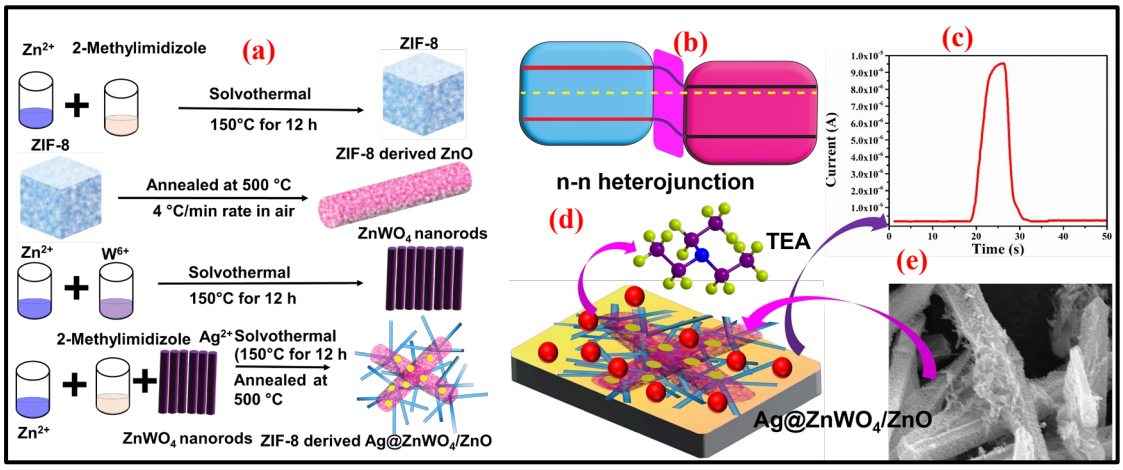

Fig. 6. Schematic representation of (a) synthesis process of ZIF-8 MOF, ZnO, $ZnWO_4$, and Ag@$ZnWO_4$/ZnO heterostructure, (b) band diagram of n-n heterojunction (c) TEA gas sensing mechanism (d) transit TEA sensing for 5 ppm at 80°C, and (e) SEM micrograph ofAg@$ZnWO_4$/ZnO heterostructure.

The optical band gap and absorption of synthesized nanomaterial were investigated by using UV-visible spectroscopy. The direct optical band gaps of ZIF-8, ZnO, $ZnWO_4$, and Ag@$ZnWO_4$/ZnO were found as 4.42 eV, 3.41 eV, 3.69 eV, and 3.51 eV respectively. The TEA gas sensing characteristics are examined towards various concentrations (1-35 ppm). The TEA gas sensing mechanism and transit sensing curve at 5 ppm of Ag@$ZnWO_4$/ZnO heterostructure sensors are shown in Fig.

6(b, c). The Ag@$ZnWO_4$/ZnO sensor demonstrated ultra-high response of 56.15 to 5 ppm at 80°C, which is 3.86, 3.14, and 1.83 times higher than from pristine ZIF-8, ZnO and $ZnWO_4$ respectively. Also, the rapid response and recovery times of 1.02 s and 1.26 s were observed towards 1 ppm of TEA. Furthermore, the fabricated sensor had reliable consistency, excellent repeatability, and long-term stability. Remarkably, the developed Ag@$ZnWO_4$/ZnO sensor revealed more prominent sensing characteristics compared with ZIF-8, ZnO and $ZnWO_4$ sensors towards low-trace of Triethylamine (TEA) at 80°C. The hierarchical structure and n-n heterojunction of Ag@$ZnWO_4$/ZnO, which create more active sites for the adsorption of oxygen and target gases and expand the possibilities for reactions between the chemisorbed oxygen species and TEA, are responsible for the significant improvement of the sensing characteristics. The preparation idea described in this work might provide a flexible platform utilized for various composite sensing material-based branched heterostructures.

Chapter 7 gives the concluding remarks and comparative analysis of all synthesized materials and fabricated devices. This chapter deals with the summarised information on the material characteristics, sensing output, and future scope of all the chapters mentioned previously. A chapter-wise overview of this thesis including the materials and their sensing performance is depicted in Table 7.1 as follows:

Table 7.1 Chapter-wise information and characteristics of developed material and sensor.

Chapter No.	**Materials**	**Method**	**Analytes**	**Detection range**	**Response**	**T_{res} (sec)**	**T_{res} (sec)**	**Sensitivity**	**Temp. (°C)**	**Porosity (%)**
1.	Introduction and aim of research work									
2.	In/SnO_2	Sol-gel	LPG	0.5/2.0 vol%	1.53/4.65	10-32	14/27	2.087	28	13.16
3.	ZnO/NiO	Green	LPG	0.5-2.0 vol%	2.30/7.72	7/27	11/30	2.69	28	19.19
4.	SnO_2@CdO	Hydrothermal	CO_2 (Dark)	200-1400 ppm	2.18/4.05	8/42	10/47	0.00153	30	23.37
			CO_2 (Light)		4.20/10.67	6.16/18.53	8.06/21.03	0.00516		
5.	CeO_2/CdS	Hydrothermal	CO_2 (Resistive)	250-1000 ppm	1.33/3.62	4.82/12.53	6.39/20.23	0.0032	30	18.65
			CO_2 (Self-powered)	250-1000 ppm	5-30	1.835	0.820	0.034		
6.	Ag@$ZnWO_4$/ZnO	Solvothermal	TEA	5-35 ppm	56.13/470.78	3.29/8.83	4.06/9.84	13.78	80	28.46
7.	Concluding remark and future scope of research									

Future scope and challenges

- Many new and unique types of metal oxide gas sensors are being constructed from nano-heterostructures because of their high surface-to-volume ratio that amplifies the above effect. Typically, heterostructures are core-shell, decorated, branched, and multi-layered thin films. However, the recent surge of interest and research in nano heterostructure has promised to increase many unique hierarchical designs and capable enhancement of properties. The electron interaction and charge transportation between component materials/structures are the most important parameters for understanding sensor behaviour. The dopant oxides can be used to control the microstructure or morphology of the materials, which further modifies electronic states.

- Certain new techniques are enabling the characterization of the nano heterostructures, significantly refining the consideration of the electronic properties. STEM-VEELS (valance electron energy-loss spectroscopy) have the potential to particularly obtain the bandgap of the secondary materials deposited onto the nanowires and state the modulation induced by processing approaches. STEM-CL (cathodoluminescence) has the potential to calibrate the energy levels and spatial variations of mid-gap defects along with the bandgap in direct-gap materials. Both approaches can be employed before and after the exposure to the coated substrates towards the investigation. XPS (x-ray photoelectron spectroscopy) may be employed for determining the band edge offset between the multiple semiconducting materials present in a nano heterostructure which confirms the movement of charge carriers across the interface due to Fermi level equilibrium.
- Self-powered gas sensors are able to work independently without the need for external power generation or supply systems because of two innovative aspects: PENG and TENG.
- The piezo-tribo hybrid nanogenerator-based self-powered gas sensing devices may be developed in future.
- This class of self-powered gas sensors will have outstanding sensitivity, best selectivity, high reliability, and extended lives for a variety of conditions and applications.

References

[1] I. Manisalidis, E. Stavropoulou, A. Stavropoulos, E. Bezirtzoglou, Environmental and health impacts of air pollution: a review, Frontiers in public health 8 (2020) 14.

[2] Y. Jian, W. Hu, Z. Zhao, P. Cheng, H. Haick, M. Yao, W. Wu, Gas sensors based on chemi-resistive hybrid functional nanomaterials, Nano-Micro Letters 12 (2020) 1-43.

[3] Y. Yan, C. Wladyka, J. Fujii, S. Sockanathan, $Prdx_4$ is a compartment-specific H_2O_2 sensor that regulates neurogenesis by controlling surface expression of GDE_2, Nature communications 6(1) (2015) 7006.

[4] G. Korotcenkov, Handbook of gas sensor materials, Conventional approaches 1 (2013).

[5] N. Joshi, T. Hayasaka, Y. Liu, H. Liu, O.N. Oliveira, L. Lin, A review on chemiresistive room temperature gas sensors based on metal oxide nanostructures, graphene and 2D transition metal dichalcogenides, Microchimica Acta 185 (2018) 1-16.

[6] A. Singh, K. Kumar, S. Sikarwar, B. Yadav, Highly sensitive and selective LPG sensor working below lowest explosion limit (LEL) at room temperature using as-fabricated indium doped SnO_2 thin film, Materials Chemistry and Physics 287 (2022) 126275.

[7] B. Huang, Y. Li, W. Zeng, Application of Metal-Organic Framework-Based Composites for Gas Sensing and Effects of Synthesis Strategies on Gas-Sensitive Performance, Chemosensors 9(8) (2021) 226.

[8] A.T. Güntner, N.J. Pineau, P. Mochalski, H. Wiesenhofer, A. Agapiou, C.A. Mayhew, S.E. Pratsinis, Sniffing entrapped humans with sensor arrays, Jounral of Analytical chemistry 90(8) (2018) 4940-4945.

[9] M. Righettoni, A. Amann, S.E. Pratsinis, Breath analysis by nanostructured metal oxides as chemo-resistive gas sensors, Materials Today 18(3) (2015) 163-171.

[10] A. Singh, S. Sikarwar, A. Verma, B.C. Yadav, The recent development of metal oxide heterostructures based gas sensor, their future opportunities and challenges: a review, Sensors and Actuators A: Physical 332 (2021) 113127.

[11] Y. Liu, S. Xiao, K. Du, Chemiresistive Gas Sensors Based on Hollow Heterojunction: A Review, Advanced Materials Interfaces 8(12) (2021) 2002122.

[12] S. Ghotekar, H. Dabhane, P. Tambade, V. Medhane, Plant-based green synthesis and applications of cuprous oxide nanoparticles, Handbook of Greener Synthesis of Nanomaterials and Compounds, Elsevier2021, pp. 201-208.

List of publications

Publications included in Thesis

1. **Ajeet Singh,** Samiksha Sikarwar, Arpit Verma, and Bal Chandra Yadav, The recent development of metal oxide heterostructures based gas sensor, their future opportunities, and challenges: a review, Sensors and Actuators A: Physical 332 (2021) 113127.
2. **Ajeet Singh,** Kuldeep Kumar, Samiksha Sikarwar, and B. C. Yadav. "Highly sensitive and selective LPG sensor working below lowest explosion limit (LEL) at room temperature using as-fabricated indium doped SnO_2 thin film, Materials Chemistry and Physics 287 (2022) 126275.
3. **Ajeet Singh,** and Bal Chandra Yadav, Green synthesized ZnO/NiO heterostructures based quick responsive LPG sensor for the detection of below LEL with DFT calculations, Results in Surfaces and Interfaces 11 (2023) 100103**.**
4. **Ajeet Singh**, and B. C. Yadav, Photo-responsive highly sensitive CO_2 gas sensor based on SnO_2@ CdO heterostructures with DFT calculations, Surfaces, and Interfaces 34 (2022) 102368. **I.F. = 6.137.**
5. **Ajeet Singh**, Shakti Singh, B. C. Yadav, Gigantic enhancement in response of heterostructured CeO_2/CdS nanospheres based self-powered CO_2 gas sensor: A comparative study, Sensors and Actuators B: Chemical 377 (2022) 133085.
6. **Ajeet Singh** and B. C. Yadav, Extremely Responsive and Selective Triethylamine Sensor based on ZIF-8 derived Ag sensitized $ZnWO_4$/ZnO Branched Heterostructures **(under review).**

Publication not included in Thesis

1. **Ajeet Singh**, Samiksha Sikarwar, and B. C. Yadav, Design and fabrication of quick responsive and highly sensitive LPG sensor using ZnO/SnO_2 heterostructured film, Materials Research Express 8, no. 4 (2021) 045013.
2. **Ajeet Singh**, Shakti Singh, B. C. Yadav, In_2O_3 Nanocubes and $ZnWO_4$ Nanorod based Triboelectric Nanogenerator for Self-Powered Humidity Sensors, Sensors and Actuators B: Chemical.
3. **Ajeet Singh**, Arpit Verma, and B. C. Yadav, MnO_2-SnO_2 based liquefied petroleum gas sensing device for lowest explosion limit gas concentration, ECS Sensors Plus 1, no. 2 (2022): 025201.

4. **Ajeet Singh**, Sanjay Kumar Yadav, Arpit Verma, Samiksha Sikarwar, and Bal Chandra Yadav, Hydrothermally Synthesized $ZnSnO_3$ Nanoflakes Based Low-Cost Sensing Device for High Performance CO_2 Monitoring, *ECS Advances* 2 (2023) 016501.
5. **Ajeet Singh**, Samiksha Sikarwar, and Bal Chandra Yadav, Metal-Organic Frameworks for Gas Sensors, In Smart Nanostructure Materials and Sensor Technology, pp. 225-244. Springer, Singapore, 2022.
6. **Ajeet Singh**, Roop Kishor, Ram Naresh Bharagava, and Bal Chandra Yadav, Existing and Emerging Treatment Technologies for the Degradation and Detoxification of Textile Industry Wastewater for the Environmental Safety, In Bioremediation, pp. 1-13. CRC Press, 2022.
7. Kuldeep Kumar, **Ajeet Singh**, Utkarsh Kumar, Ravi Kant Tripathi, and B. C. Yadav, The beauty inhabited inside the modified Graphene for moisture detection at different frequencies, Journal of Materials Science: Materials in Electronics 31, no. 13 (2020) 10836-10845.
8. Zaireen Fatima, Chandkiram Gautam, **Ajeet Singh**, Sarvesh Kumar Avinashi, Bal Chandra Yadav, and Afroj Ahmed Khan, Fabrication of a novel nanocomposite SiO_2-H_3BO_3-V_2O_5-Al_2O_3 via melt-quenching technique: structural and surface morphological characteristics for carbon dioxide gas sensing applications, Journal of Materials Science: Materials in Electronics 33 (2021) 1192-1210.
9. Sarvesh Kumar Gupta, Abhishek Kumar Gupta, Rajesh Kumar Yadav, **Ajeet Singh**, and B. C. Yadav. Highly efficient in-situ sulfur doped graphitic carbon nitride nanoplates as an artificial photosynthetic system for NADH regeneration, Vietnam Journal of Chemistry 59, no. 5 (2021): 590-598.
10. Shivani Gupta, Rajesh K. Yadav, Abhishek Kumar Gupta, **Ajeet Singh,** B. C. Yadav, and Brijesh K. Pandey, One-Pot Highly Efficient Synthesis of N-Enrich Graphene Quantum Dots as a Photocatalytic Platform for NAD^+/$NADP^+$ Reduction, Photochemistry and Photobiology 97, no. 6 (2021) 1498-1506.
11. Sarvesh Kumar Gupta, Abhishek Kumar Gupta, Rajesh Kumar Yadav, **Ajeet Singh**, and Bal Chandra Yadav, Highly efficient S-g-CN/Mo-368 catalyst for synergistically NADH regeneration under solar light, Photochemistry and Photobiology 98, no. 1 (2022): 160-168.

12. Zaireen Fatima, Chandkiram Gautam, **Ajeet Singh,** Sarvesh Kumar Avinashi, Bal Chandra Yadav, and Afroj Ahmed Khan. "Synthesis of a porous SiO_2-H_3BO_3-V_2O_5-P_2O_5 glassy composite: structural and surface morphological behaviour for CO_2 gas sensing applications. *RSC advances* 12, no. 49 (2022): 31585-31595.
13. Arpit Verma, Priyanka Chaudhary, **Ajeet Singh**, Ravi Kant Tripathi, and B. C. Yadav. ZnS Nanosheets in a Polyaniline Matrix as Metallopolymer Nanohybrids for Flexible and Biofriendly Photodetectors, ACS Applied Nano Materials 5, no 4 (2022) 4860-4874.
14. Preeti Dixit, Shweta, **Ajeet Singh**, Sarvesh Kumar Avinashi, Bal Chandra Yadav, and Chandkiram Gautam, Fabrication, structural, and physical properties of alumina doped calcium silicate glasses for carbon dioxide gas sensing applications, Journal of Non-Crystalline Solids 583 (2022): 121475.
15. Priyanka Chaudhary, **Ajeet Singh**, Samiksha Sikarwar, and B. C. Yadav. "One-pot synthesis of phosphine-free indium selenide (InSe) QDs and their structural characterization for LPG and humidity sensing. Journal of Materials Science: Materials in Electronics 33, no. 15 (2022): 11802-11812.
16. Arpit Verma, Deepankar Yadav, **Ajeet Singh**, Monu Gupta, K. B. Thapa, and B. C. Yadav, Detection of acetone via exhaling human breath for regular monitoring of diabetes by low-cost sensing device based on perovskite $BaSnO_3$ nanorods, Sensors and Actuators B: Chemical 361 (2022): 131708.
17. Arpit Verma, Priyanka Chaudhary, Ravi Kant Tripathi, **Ajeet Singh**, and B. C. Yadav, State of the Art Metallopolymer Based Functional Nanomaterial for Photodetector and Solar Cell Application, Journal of Inorganic and Organometallic Polymers and Materials 32 (2022): 1-20.
18. Samiksha Sikarwar, Anwesh Pandey, **Ajeet Singh**, B. C. Yadav, I. E. Uflyand, and G. I. Dzhardimalieva, Synthesis of La_2O_3-Cr_2O_3-SrO nanocomposite by pyrolysis of metal carboxylates; its characterization, DFT studies and significance in humidity sensing, Materials Science and Engineering: B 283 (2022) 115813.
19. Vernica Verma, N. K. Pandey, **Ajeet Singh**, Peramjeet Singh, Priya Gupta, and B. C. Yadav, Liquefied petroleum gas (LPG) sensing of biphasic Cu_6Sn_5:SnO_2 nanocomposite thin-films, Materials Chemistry and Physics 289 (2022) 126459.

20. Monu Gupta, Priyanka Chaudhary, **Ajeet Singh**, Arpit Verma, Deepankar Yadav, and B. C. Yadav, Development of MoO_3-CdO nanoparticles-based sensing device for the detection of harmful acetone levels in our skin and body via nail paint remover, Sensors and Actuators B: Chemical 368 (2022) 132102.
21. V. Manikandan, S. Vigneselvan, Iulian Petrila, Rajaram S. Mane, **Ajeet Singh**, Kamil Sobczak, and J. Chandrasekaran, Long-lasting stability and low-concentration SO_2 gas detection aptitude of Sn-doped alumina sensors, Materials Chemistry and Physics 291 (2022) 126691.
22. Prabhakar Yadav, **Ajeet Singh,** Shakti Singh, Dheeraj Kumar Shukla, Design, and development of Paper/ZnO-SnO_2 heterostructured Ultra-Fast TENG based LPG sensor, ECS Sensor plus, 1 (2022) 042601.
23. Peramjeet Singh, N. K. Pandey, VV Siva Kumar, Vernica Verma, **Ajeet Singh**, Priya Gupta, and B. C. Yadav. Highly sensitive pure molybdenum trioxide thin films at a higher annealing temperature for liquefied petroleum gas and humidity sensing at room temperature. Applied Physics A 129, no. 4 (2023): 250.
24. Maikesh Mathur, Arpit Verma, **Ajeet Singh**, B. C. Yadav, and Vishal Chaudhary, $CuMoO_4$ nanorods-based acetone chemiresistor-enabled non-invasive breathomic-diagnosis of human diabetes and environmental monitoring, Environmental Research 229 (2023) 115931.
25. Aastha Singh, **Ajeet Singh**, Arpit Verma, Bal Chandra Yadav, and Vishal Chaudhary. Economic $ZnCo_2O_4$ Nanoflakes Chemiresistor Assisted Room-Temperature Monitoring of Low Trace Airborne Ammonia, ECS Journal of Solid-State Science and Technology 12, no. 4 (2023): 047005.
26. Navin Chaurasiya, **Ajeet Singh,** Kuldeep Kumar et al. Highly sensitive room temperature liquid petroleum gas (LPG) sensor with fast response based on titanium di oxide (TiO_2)-reduced graphene oxide (r-GO) composite, *Sensors & Diagnostics* (2023).

Papers presented in National and International Conference/Webinar/Workshop

1. National Symposium on "Advanced Materials Science (NSAMS)" held on 7th – 8th December 2018 in DDU Gorakhpur, U.P., India. **(Poster Presentation).**
2. National conference on "Sukshm Padarth evam Sambaddh Chetan Urja" held on 1st – 3rd February 2019 in BBAU Lucknow, U.P., India. **(Poster Presentation).**
3. Workshop on Important Techniques for Characterization of Molecules" held on 25th – 31th March 2019 in SRM University Lucknow U.P., India. **(Participate).**
4. National Conference on "Recent Advances in Chemical Sciences (NCRACS)" held on 29th -30th March 2019 in MMM University of Technology, Gorakhpur, U.P., India. **(Poster Presentation).**
5. International Conference on "Ultrasonic and Material Science for Advance Technology" held on 16th -18th November 2019 in VBSPU Jaunpur, U.P., India. **(Poster Presentation).**
6. International Webinar on Nanoscience and Nanotechnology (IWNN-2020), 27th – 29th November, 2020, BBAU, Lucknow **(Oral presentation)**.
7. "Synergistic Training Utilising the Scientific and Technological Infrastructure" (STUTI) training workshop, 22-28 August, 2022, BBAU, Lucknow **(Workshop).**

Achievements

- **Best Research Excellence Award 2022** at Babasaheb Bhimrao Ambedkar University, Lucknow.
- **Best oral presentation award** in National Science Day Conference "Global Science for Global wellbeing" organized by Department of Physics, Babasaheb Bhimrao Ambedkar University, Lucknow.

Patent

C. R. Gautam, S. K. Avinashi, Shweta, S. Kumari, R. K. Mishra, Rakhi, A. Sachan, Z. Fatima, A. Hussain, A. Gautam, **Ajeet Singh**, B. C. Yadav, "Fly ash doped clay ceramic nanocomposite, its preparation method and sensor", **Application No. 202311064285**